Robot-LDA plane measurements and smoke investigations on a 30° inclined flat plate in an open wind channel with and without plasma actuation effect

Manuel Berger[1,*], Martin Wilhelm[2], Leonhard Güntner[2], Christian Mayerl [3], Tobias Kofler [3], Thomas Senfter[3], Lukas Zingerle[3], Martin Pillei[3]

1: Dept. of Medical Technologies, MCI - The Entrepreneurial School, Austria
2: Dept. of Environmental, Process & Energy Engineering, MCI - The Entrepreneurial School, Austria
3: Dept. of Industrial Engineering & Management, MCI - The Entrepreneurial School, Austria
*Corresponding author: manuel.berger@mci.edu

Keywords: laser Doppler anemometry, ABB robot, smoke investigations, plasma actuation effect, 30° inclined flat plate.

ABSTRACT

Active flow control is a relatively new approach to influence the velocity vector field for plane airfoils or process engineering applications with a plasma source. The goal is to positively effect the point of separation to increase the lift/drag ratio or increase separation efficiency and to reduce pressure drop. In the presented study two approaches, the Robot-LDA measurements and smoke investigations, are chosen to find out whether the plasma source has an effect on the velocity vector field on a 30° inclined flat plate and the separation point. A flow rate of 250 m³/h resulting in a Reynolds number of 100 000 is chosen, since this is typical for already presented results within the field of plasma source investigations. With Robot-LDA in total 825 measurements points of the axial wind channel velocity components are captured twice, with and without activated plasma source. The measurement plane was set 80 mm x 50 mm orthogonal to the flat plate in the middle of the wind channel axis. The plasma source was powered with $14\ \mathrm{kV_{p-p}}$ and 5 kHz. Due to stability of the plasma actuator, the LDA measurements were subdivided into eight regions. For the same configurations smoke investigations are performed. A chromium-nickel wire with a diameter of 0.213 mm is heated by an electronic circuit including capacitor and power source to vaporize liquid paraffin. The flow field is captured by a highspeed camera.

Robot-LDA measurement results show a free-stream axial wind channel velocity component of about 15 m/s. In the shadow region of the 30° inclined flat plate a recirculation zone is found due to negative velocity components. At a distance up to 12 mm close to the plat plate, wall reflections dominated and to find valid LDA measurement results were not possible. With and without activated plasma source velocity differences between -0.5 m/s and 0.5 m/s are found. The biggest velocity differences are in the region of 15 mm to 45 mm relative to the tip of the inclined flat plate. For post-processing purposes, the 3D wind channel geometry and the Robot-LDA measurement results are loaded in ParaView 5.10.1. Smoke investigations show that the plasma source minimally attach the flow to the flat plate. This effect is higher with smaller flow rates (50 m³/h) than with 250 m³/h.

Robot-LDA and smoke measurement results are promising that flow influence due to plasma has potential in various applications in future.

1. Introduction

The research within active flow control (AFC) began around ten years ago, since high voltage and high frequency dielectric barrier discharce (DBD) and the corresponding actuators were available Benard & Moreau (2014); Moreau (2007). Two electrodes with a sinusoidal high voltage separated by a layer of dielectric material are used. An electric or ionic wind is generated, at a few meters per second, and it alters the velocity vector field in the vicinity of the two electrodes Karadag et al. (2021).
In Göksel et al. (2007) the aerodynamics with DBD plasma actuator (PA) is investigated qualitatively by smoke visualization technique. Therefore, a tilted Eppler E338 airfoil is used, equipped with an electrode and investigated in the Reynolds number range from 20 500. The DBD was powered with $10\ \mathrm{kV_{p-p}}$ and 4 kHz. The tilting angle was varied between -10° to 30°. The lift coefficient is calculated based on force measurements. Results of smoke investigations show that with DBD the seperation point move in dowstream direction of the airfoil and the flow is more tangetial to the upper airfoil surface. The results of the force measurements show an about 3 times higher lift coefficient in between tilting angle of 10° to 25° and about factor 2 within 0° and 10°. The limitation of this study is the low Reynolds number.
In the references Matsunuma (2022); Zoppini et al. (2020), investigations have been conducted using two-dimensional, two-component (2D, 2C) particle image velocimetry (PIV) measurements on airfoils with dielectric barrier discharge (DBD) plasma actuators. In Zoppini et al. (2020), the DBD is mounted on the nose of a NACA 0015 airfoil with a chord of 300 mm and a span of 930 mm, operating at $40\ \mathrm{kV_{p-p}}$, 650 Hz, and 250 W. The airspeed is set to 35 m/s, resulting in a Reynolds number of 700 000. At angles of attack of 14.5° and 22°, a disparity in the two-dimensional velocity vector field is observed between the DBD being switched on and off, with different measurement planes along the model. With the DBD activated, the flow adheres more closely to the airfoil profile, and the stall is shifted downwards in the direction of flow. The plasma discharge exhibits varying effects: in the central zone, it reduces the size of the recirculating region and shifts the stall downstream, while on the outer sections, it only induces minor alterations in the local streamlines.
The most recent publication by Matsunuma (2022) forms the foundation for the presented study. Investigations were conducted at $12\ \mathrm{kV_{p-p}}$, 10 kHz, and within a low Reynolds number range of 18 000 to 37 000. Experimental findings suggest that the DBD should be installed on the leading edge, facing the flow. This positioning allows for acceleration of the inlet boundary layer before the leading edge weakens the horseshoe vortex, thereby influencing the initial formation of the through vortex. A detailed quantitative analysis reveals a -48% and -59% shift in the position of the main vortex. The impact on the flow field diminishes as the Reynolds number increases.
In the presented study, an ABB robot with a 1D-LDA is used to investigate 825 measurement points of the fuselage plate flow with and without the DBD switched on. The planning of the robot movement is done by ABB RobotStudio®. For this purpose, a plug-in has been developed in two master theses Hausberger (2017); Sieberer (2021), which are used. At LXLaser 2022 this plug-in was already presented to perform measurements in an open wind channel and an ellipsoid Berger et al.

(2022). Compared to the already existing investigations, the LDA has a higher temporal resolution compared to the PIV or the smoke studies. However, for simplicity, a 30° inclined plate with cross-sectional dimensions of 46 mm x 4 mm is investigated rather than a NACA profile. The width of the plate is 280 mm. The measurements have been made in the center, i.e. at 140 mm. The open wind tunnel has an inlet diameter of 80 mm. Additionally, smoke investigations are investigated as well. A chromium-nickel wire with a diameter of 0.213 mm is heated by an electronic circuit including capacitor and power source to vaporize liquid paraffin. The flow field is captured by a highspeed camera. The orthogonal distance to the inclined flat plate is measurement in pixel coordinates and calculated to physical coordinates.

2. Methods

2.1. LDA measurements - Experimental setup

Fig. 1 illustrates the experimental setup. The LDA ILA fp50, equipped with a 250 mm lens (2), is mounted on the ABB robot IRB 1200 7kg 0.7m (1). The ILA LDA control systems qt 2.0.10 (6) is utilized for data acquisition of the LDA measurement results. The programmed plug-in is installed in RobotStudio® version 2021 (7). The open wind channel (4) is adjusted to a flow rate of 250 m^3/h, corresponding to a Reynolds number of 100 000. The channel is equipped with a 30° inclined flat plate (3) with cross-sectional dimensions of 46 mm x 4 mm and a width of 280 mm. As suggested by Matsunuma (2022), the DBD is positioned at the tip of the blade. The copper electrodes have a width of 5 mm at the top of the plate and 15 mm at the bottom, situated 5 mm below the top edge. An overlap of 0.5 mm between the top and bottom sections is maintained. The voltage for all measurements is set to $14\ \mathrm{kV_{p-p}}$, with a frequency of 5 kHz. The measurement area of interest is orthogonal to the plate (top side) and spans 80 mm x 50 mm. Due to ozone exposure and limited time stability of the DBD, this area is divided into eight subareas of 10 mm x 50 mm. Fig. 2 shows the 30° inclined plate with DBD, along with the activated LDA. The robot control unit (5) is responsible for the control of the ABB robot. The teach pendant, not depicted in Fig. 1, is employed for pre-processing. Subsequently, the robot is switched to automatic mode for conducting the measurements. The LDA raw signal processing unit (8) includes hardware filters to preprocess the signal, enhancing the signal-to-noise ratio, and ultimately evaluating the velocity component within the ILA LDA control systems qt 2.0.10. Components (9-11) are associated with plasma generation and monitoring. In (9), the high-voltage power supply is located. A storage oscilloscope is employed to monitor the voltage while the DBD is active, as the sinusoidal shape may change before the actuator burns out. Since the high-voltage source alone cannot generate a signal, this task is carried out by the function generator (11).

Figure 1. Experimental setup - LDA measurements: (1) ... robot ABB IRB 1200 7kg 0.7m, (2) ... LDA ILA fp50-shifted, (3) ... 30° inclined flat plate, (4) ... open wind channel, (5) ... robot control unit, (6) ... LDA measurement PC for post-processing, (7) ... Laptop with ABB RobotStudio®2021 to control the robot, (8) ... LDA raw signal processing including hardware filters, (9) ... high voltage power supply TRek 20/20C-HS, (10) ... scope Tektronik TDS 2002C, (11) ... function generator Agilent 33250A. The additional equipment used for smoke investigation is not shown. Fig. is taken from Berger et al. (2023).

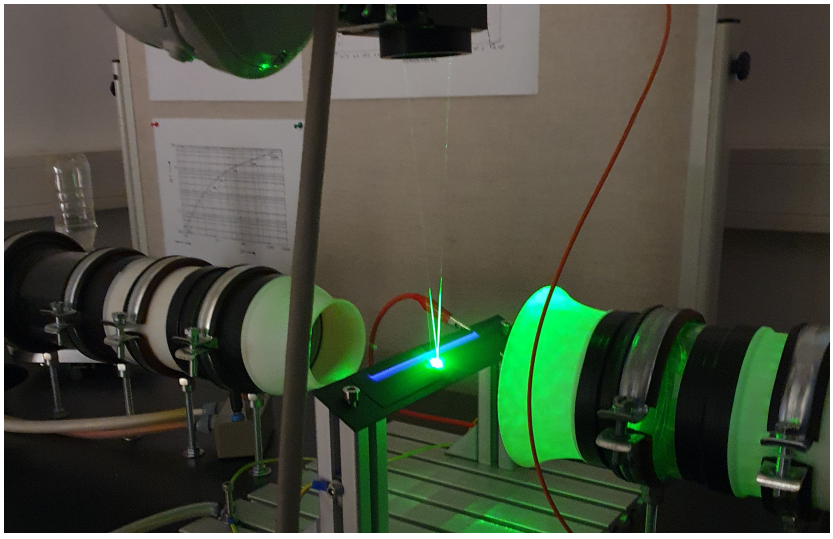

Figure 2. Experimental setup - LDA measurements. Photo during measurement with LDA switched on, wind tunnel, DBD and seeding. Figure is taken from Berger et al. (2023).

The LDA software parameter were defined to achieve high mount of valid bursts, resulted in a sampling frequency = 50 MHz, Number of smaples = 512, band pass filter = 100 kHz - 20 MHz and a burst validation factor = 3. Each measurement point was investigated in between 10 seconds and 15 seconds. The seeding droplets consisted of di(2-ethylhexyl)sebacate (DEHS) with a modal diameter of about 1.2 µm and a Stokes number smaller than 1, so that the droplets followed the air without any delay.

When the DBD is switched on, ozone is generated which is harmful to health. For this reason, 3M 9928 FFP2 protective masks with activated carbon filters was used during all measurements. Since the high voltage at the DBD is potentially dangerous, a distance of 1 m was always maintained.

2.2. LDA measurements - Points and path planning

The points and path planning is performed as presented in Berger et al. (2022). The origin and the measurement coordinate system is defined at the top left corner of the plate, which is used for registration of the real model and the planned digital twin within RobotStudio®. The measurement region with the size 80 mm x 50 mm orthogonal to the plate and in the middle of the wind is split up into eight regions. The number of measurement points are from surface (1) to (8), see. Fig. 3, 128, 121, 120, 124, 123, 127, 125 and 124. The Auto Configuration path planning option is used. The tool center point (TCP) of the LDA is calibrated by three points (point 1: x1, point 2: x2, point 3: y1). The z-axis is automatically calculated. The measurement points are evaluated with switched on and switched off DBD.

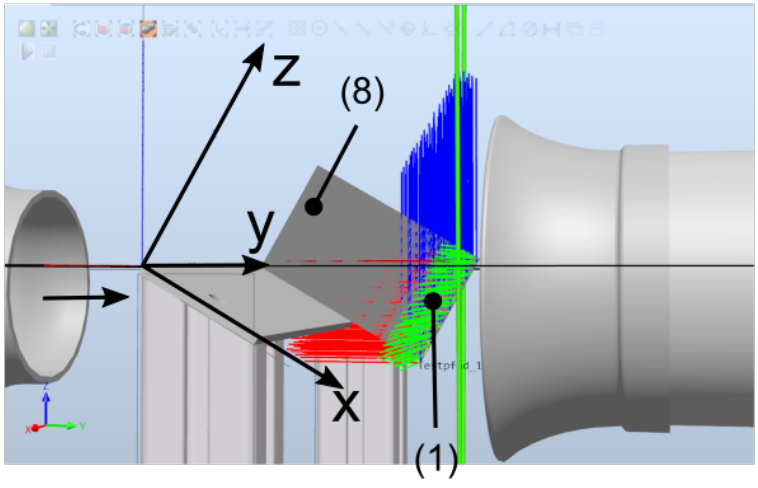

Figure 3. Point and path planning within ABB RobotStudio®software. The lines (red, green and blue) show the pose of every measurement point consisting position and orientation. The flow direction is from left to right. Figure is partly taken and adapted from Berger et al. (2023).

2.3. Smoke measurements

Smoke measurements were performed based on Gao & Liu (2018). To achieve better smoke behavior, the capacity was changed from $4400\ \mu\mathrm{F}$ to $6600\ \mu\mathrm{F}$. Paraffine oil was vaporized at the chromium-nickel wire with a diameter of 0.213 mm and a length of 103 mm. The wire is mounted with a distance of 14.7 mm from the wind channel examination volume inlet. Current flows through the wire with pulses, causing it to glow. Therefore, the applied oil thus evaporates abruptly. A wire is powered with a DC voltage source with U = 68 V and a current of I = 3.0 A (MANKADF WPS1203 H). The capacitor circuit permits instantaneous electrical energy supply. The evaporated oil is illuminated with two lamps Manfrotto LYKOS bi-color and captured with the high speed camera Phantom Miro M310 with the lens Nikon DX AF-S NIKKOR 35 mm 1:1.8 G. The lens is oriented so that the front and rear edges of the and the rear edge of the holder are in alignment. The software PCC Phantom is used to calibrate the system. The image is focused in the center of the plate so that the vapor of the paraffin oil. The exposure of the camera lens is set to level 2 of 9, starting from full exposure. To highlight the vaporized paraffine oil, a dark background is chosen. The images are taken with a pixel resolution of 1280 x 800, an exposure time of 312 μs, a frame rate of 2800 fps and a duration of 0.066 s. In Fig. 4 the measurement setup for smoke visualization is shown. The camera system is not shown. For post-processing of the raw camera data the software PCC Photome was used.

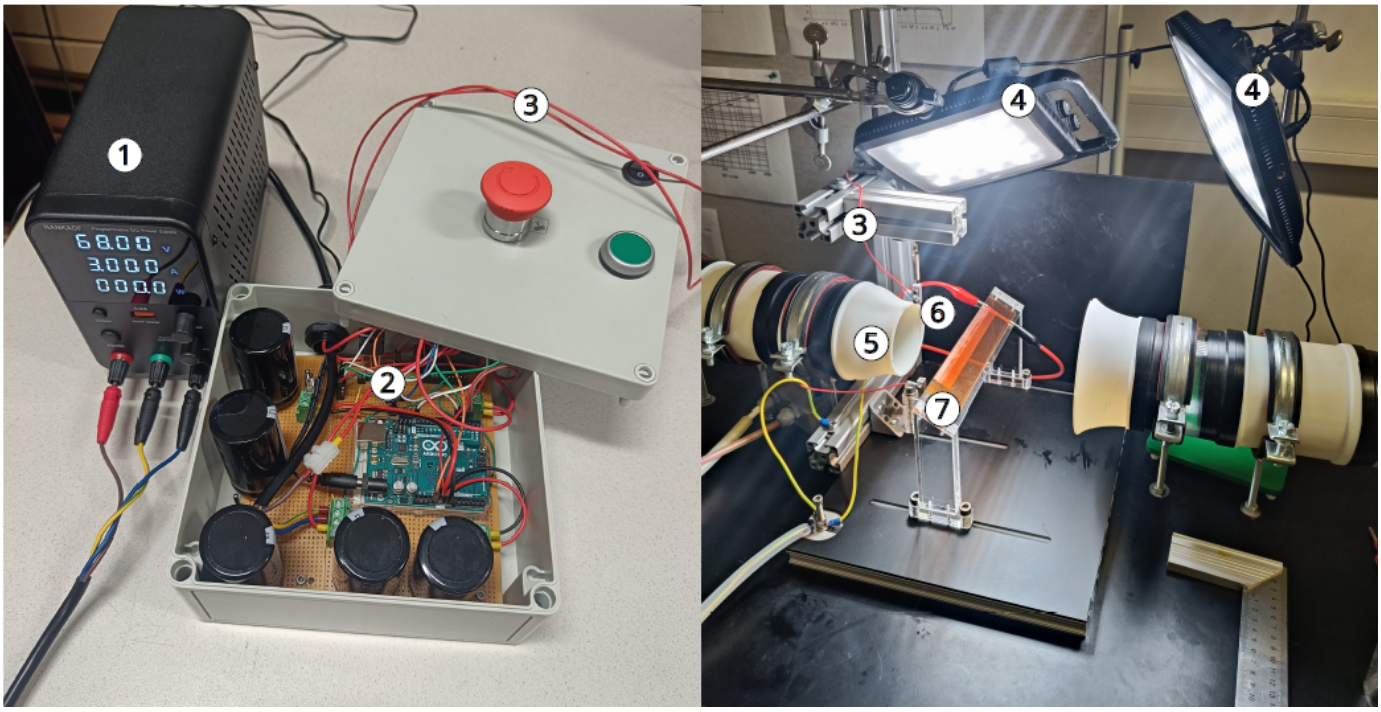

Figure 4. Experimental setup - smoke measurements: (1) ... Power Supply NANKADF WPS1203H, (2) ... condensator circuit based on Gao & Liu (2018), (3) ... cable from condensator circuit to wire, (4) ... lamps Manfrotto LYKOS bi-color, (5) ... wind channel, (6) ... NiCr wire, d = 0.2 mm, l = 103 mm. (7) ... 30° inclined flat pate. Figure is taken from Güntner (2023)

3. Results

3.1. Results of the robot-LDA measurement

Fig. 5 shows the LDA measurement results without DBD in (a) and (b) and with DBD in (c) and (d). In (a) and (c), the axial-parallel velocity component from wind tunnel is shown. (b) and (d) shows the graph of associated valid bursts for each individual measurement point. Each measurement point is shown with a triangle. The scalar field for velocity and the valid points is created by interpolation with Delaunay3D within ParaView 5.10.1. Points with less than 50 valid bursts are hidden, since laser reflection induced noise into the measurement results so that those are no usable for consideration. The result shows a backflow zone in the shadow area of the plate, which is visible by points with negative velocity component. No velocity difference is visible between (a) without DBD and (c) with DBD. Therefore the difference plot has been created (e). Here a velocity difference between -0.5 m/s and 0.5 m/s is visible. Especially in the shadow area of the plate, where the velocity is -5 m/s, the difference is even about 10%. The largest relative difference is in the middle region of the plate. From (b) and (d) it can be seen that in almost all measurement points more than 1000 valid bursts per measurement point were achieved. The transparency in ParaView for the STL file is set to 0.28, the measurement points (triangles) to 1.0 and the color area of the scalar field to 0.69.

3.2. Results of the smoke investigation

Fig. 6 shows the results of the smoke investigations (left column: without DBD, right column with DBD). The flow rates are increasing from top to bottom with 50 m^3/h, 100 m^3/h, 150 m^3/h, 200 m^3/h, 250 m^3/h. The images show that with DBD the flow is in better contact with the 30° inclined plate. At higher flow rates (velocities) the picture is unsharp. Furthermore, the higher the flow rate the smaller is the effect of the DBD.

4. Discussion

Both, the Robot-LDA measurement and the smoke investigations show that the DBD has an influence on the velocity vector field in the vicinity region of the flat plate. At the LDA measurements a velocity difference up to $\pm$ 0.5 m/s was found at a free stream velocity of about 17 m/s, which is in maximum 3%.
For faster data generation also smoke investigations of the same (250 m^3/h) and smaller flow rates are presented here. What is clearly seen, which is also supported by all other publications is that. The higher the flow rate, the smaller is the impact of the DBD.

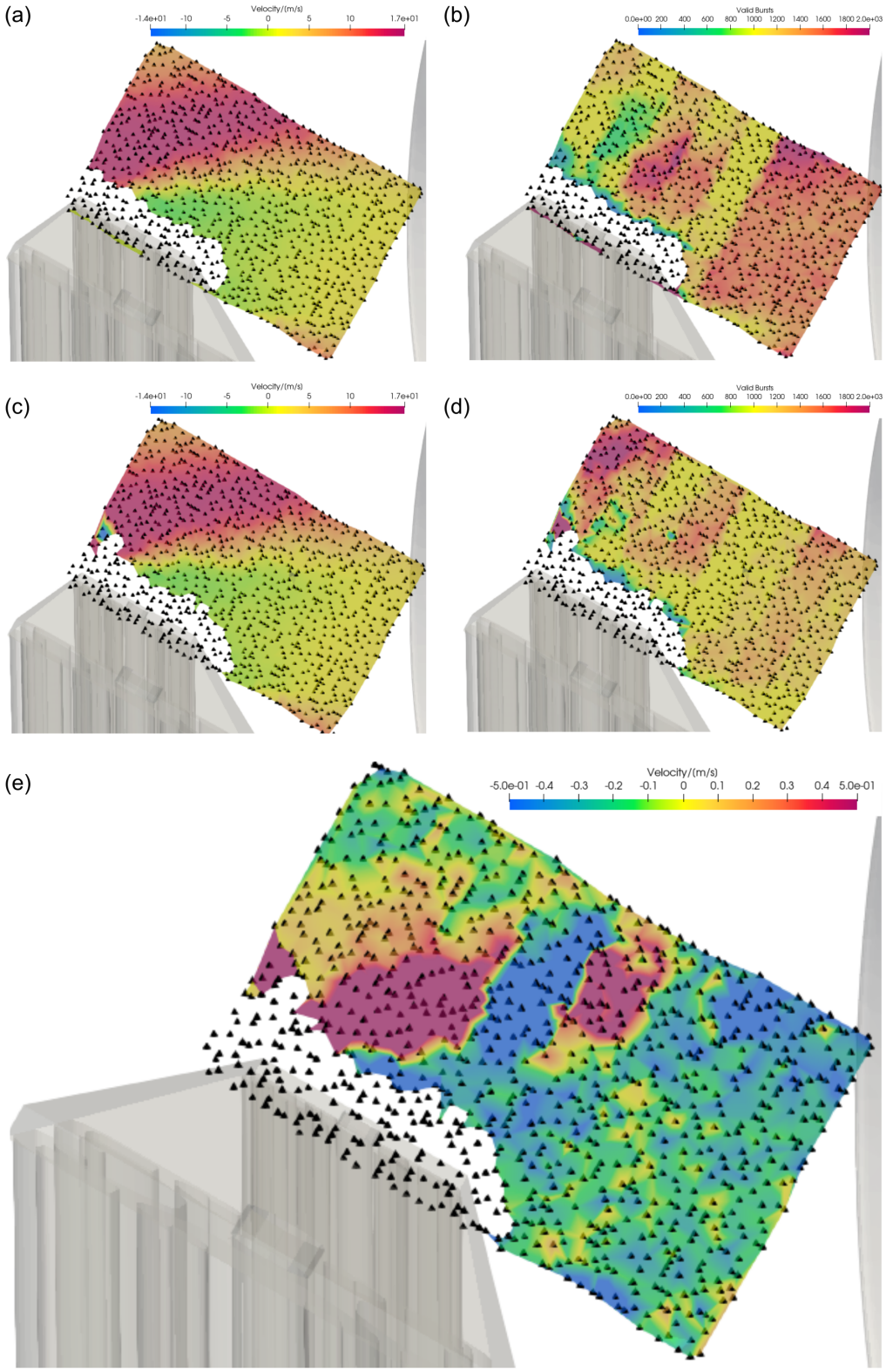

Figure 5. LDA measurement results with 3D design. The triangles show the measurement points. All scalar quantites are interpolated with Delaunay 3D within ParaView 5.10.1. The wind channel parallel axial velocity component is meaured with LDA. (a) ... velocity component without plasma, (b) ... valid bursts without plasma, (c) ... velocity component with plasma, (d) ... valid bursts with plasma, (e) ... velocity difference plot. Regions with < 50 valid bursts are not depicted. The flow rate is $250 m^3/h$. Figure is taken from Berger et al. (2023).

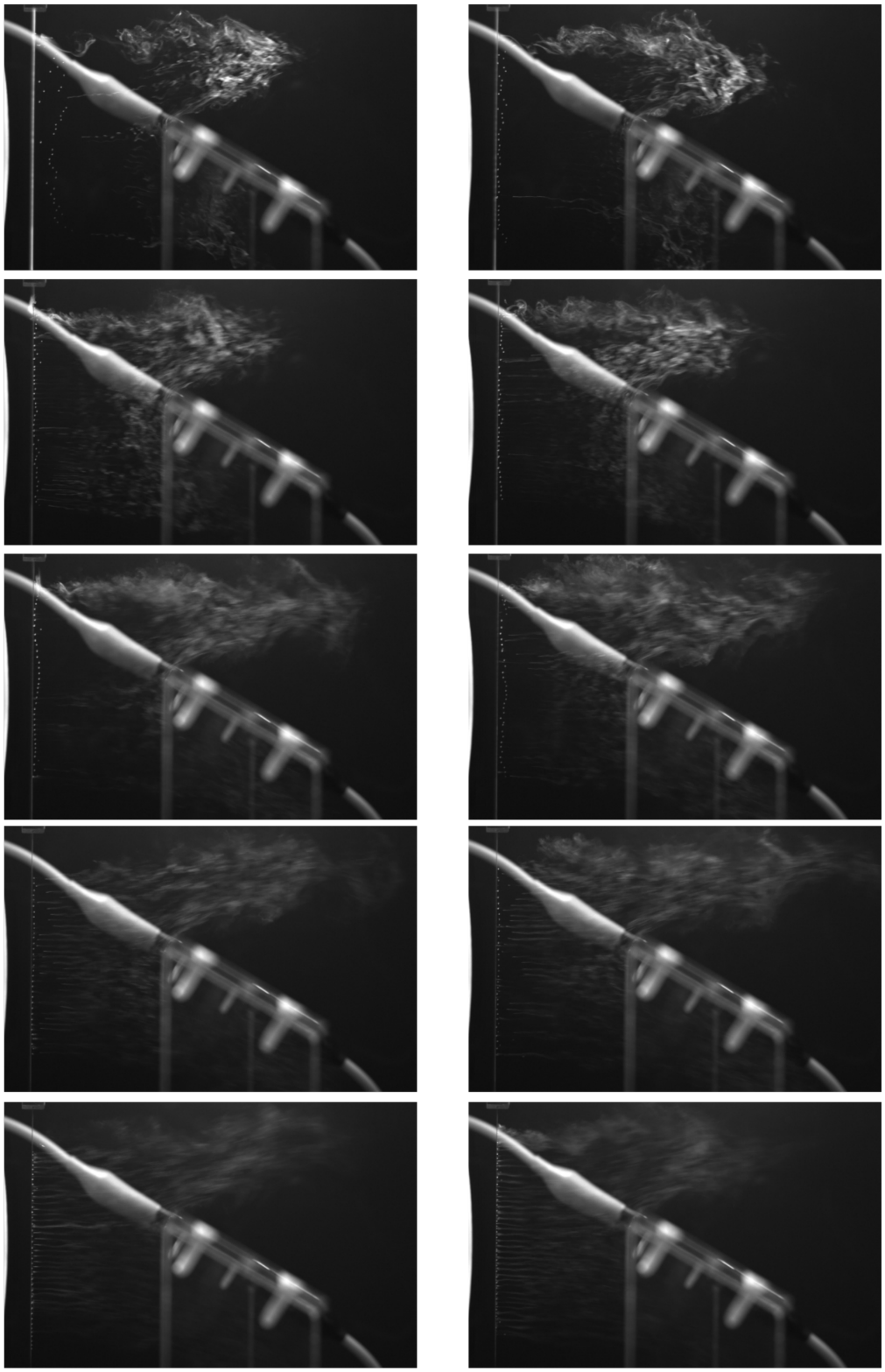

Figure 6. Smoke measurement results. Left column: without DBD. Right column: with DBD. The rows show the different flow rates: From top to bottom: 50 m^3/h, 100 m^3/h, 150 m^3/h, 200 m^3/h, 250 m^3/h. Results are taken from Güntner (2023)

References

Benard, N., & Moreau, E. (2014). Electrical and mechanical characteristics of surface ac dielectric barrier discharge plasma actuators applied to airflow control. *Experiments in Fluids*, *55*, 1–43.

Berger, M., Hausberger, T., Sieberer, J., Senfter, T., Kofler, T., Mayerl, C., … Pillei, M. (2022). Abb robotic laser doppler anemometry measurements with robotstudio with an open wind channel and an ellipsoid. *LXLaser 2022 - 20th International Symposium on Application of Laser and Imaging Techniques to Fluid Mechanics*, *20*, 848–855.

Berger, M., Wilhelm, M., Senfter, T., Mayerl, C., Kofler, T., Holzer, S., & Pillei, M. (2023). Roboterlda flächenmessungen mit einer 30° geneigten flachen platte in einem offenen windkanal mit und ohne plasmaquelle. *GALA 2023 German Association of Laser anemometry*.

Gao, N., & Liu, X. (2018). An improved smoke-wire flow visualization technique using capacitor as power source. *Theoretical and Applied Mechanics Letters*, *8*(6), 378–383.

Göksel, B., Greenblatt, D., Rechenberg, I., Kastantin, Y., Nayeri, C., & Paschereit, C. (2007). Pulsed plasma actuators for active flow control at low reynolds numbers. In *Active flow control: Papers contributed to the conference "active flow control 2006", berlin, germany, september 27 to 29, 2006* (pp. 42–55).

Güntner, L. (2023). *Optimierung der drallerzeuger von gleichstromzyklonen* [Master's thesis].

Hausberger, T. (2017). *A 6-dof laser-doppler-velocimetry system for evaluation of flow along arbitrary curved surfaces* [Master's thesis].

Karadag, B., Kolbakir, C., & Durna, A. S. (2021). Plasma actuation effect on a naca 4412 airfoil. *Aircraft Engineering and Aerospace Technology*, *93*(10), 1610–1615.

Matsunuma, T. (2022). Effects of the installation location of a dielectric barrier discharge plasma actuator on the active passage vortex control of a turbine cascade at low reynolds numbers. In *Actuators* (Vol. 11, p. 129).

Moreau, E. (2007). Airflow control by non-thermal plasma actuators. *Journal of physics D: applied physics*, *40*(3), 605.

Sieberer, J. (2021). *Flexible systems for offline planning and positioning of velocity distribution measurements* [Master's thesis].

Zoppini, G., Belan, M., Zanotti, A., Di Vinci, L., & Campanardi, G. (2020). Stall control by plasma actuators: Characterization along the airfoil span. *Energies*, *13*(6), 1374.